phosphates. Second, it seems unlikely that the small bond angle at phosphorus is necessarily the most important factor for the increased hydrolysis rates in the five-membered cyclic phosphates, inasmuch as the small angle in triphenyl phosphate does not enhance this hydrolysis rate appreciably.

Our simple consideration of the π bonding does not seem to account for the orientation of the P–O–C planes to provide maximum d–p overlap between the oxygen and phosphorus orbitals. A more complete analysis, such as that of Collins (1966), may be able to extend this treatment.

We wish to thank the National Institutes of Health for Grant GM–08395–07. We further wish to thank Montana State University for grants which have made possible some of the computing required for this study.

References

ABRAHAMS, S. C. (1950). Acta Cryst. 3, 194.
ABRAMSON, J. D. & PASCHER, I. (1966). Acta Cryst. 21, 79.
BARNARD, P. W. C., BUNTON, C. A., KELLERMAN, D., MHALA, M. M., SILVER, B., VERNON, C. A. & WELCH, V. A. (1966). J. Chem. Soc. B, p. 227.
BUNTON, C. A., KELLERMAN, D., OLDHAM, K. G. & VERNON, C. A. (1966). J. Chem. Soc. B, p. 292.

BUSING, W. R., MARTIN, K. O. & LEVY, H. A. (1962). Full Matrix Least-Squares Refinement Program ORFLS. ORNL-TM-305, Oak Ridge National Laboratory, Oak Ridge, Tennessee.
COLLIN, R. L. (1966). J. Amer. Chem. Soc. 88, 3281.
DUNITZ, J. D. & ROLLETT, J. S. (1956). Acta Cryst. 9, 327.
International Tables for X-ray Crystallography (1962). Vol. III, p. 202. Birmingham: Kynoch Press.
JOHNSON, C. K. (1965). A Fortran Thermal-Ellipsoid Plot Program for Crystal Structure Illustrations. ORNL-3794, Oak Ridge National Laboratory, Oak Ridge, Tennessee.
KRAUT, J. & JENSEN, L. H. (1961). Acta Cryst. 14, 1146.
KRAUT, J. & JENSEN, L. H. (1963). Acta Cryst. 16, 79.
NEWTON, M. G., COX, J. R. JR & BERTRAND, J. A. (1966). J. Amer. Chem. Soc. 88, 1503.
STEITZ, T. A. & LIPSCOMB, W. N. (1965). J. Amer. Soc. 87, 2488.
STOUT, G. H. & JENSEN, L. H. (1968). X-ray Structure Determination, p. 457. New York: Macmillan.
SUNDARALINGAM, M. & JENSEN, L. H. (1965). J. Mol. Biol. 13, 914.
SVETICH, G. W. & CAUGHLAN, C. N. (1965). Acta Cryst. 19, 645.
SVETICH, G. W., CAUGHLAN, C. N., LI, C. T. & WATENPAUGH, K. D. (1965). Programs for the IBM 1620. Montana State University Library.
SWANK, D., CAUGHLAN, C. N., RAMIREZ, F., MADAN, O. P. & SMITH, C. P. (1967). J. Amer. Chem. Soc. 89, 6503.

The Crystal Structure of La$_2$Sb

BY W. N. STASSEN*, M. SATO† AND L. D. CALVERT‡

Division of Chemistry, National Research Council of Canada, Ottawa, Canada

Crystals of La$_2$Sb are tetragonal, $a = 4.626$ (3), $c = 18.06$ (2) Å, $c/a = 3.904$; space group $I4/mmm$ (D_{4h}^{17}), $Z = 4$; 4 La(1) in 4(c), 0½0; 4 La(2) in 4(e), 00z with $z = 0.3204$ (2); 4 Sb in 4(e), 00z with $z = 0.1377$ (2). The structure of La$_2$Sb corresponds to two C38 structure units joined together by reflexion across a mirror plane perpendicular to the c axis. Intensities for 298 $h0l$ and $h1l$ reflexions were obtained from multiple-film Weissenberg exposures by visual comparison with a film density scale. The parameters were refined using a structure-factor least-squares program.

Introduction

The lanthanum–antimony system was first studied by Vogel & Klose (1954) who reported the phases La$_2$Sb, La$_3$Sb$_2$, LaSb and LaSb$_2$. The rock-salt structure of LaSb had already been established by Iandelli & Botti (1937). Wang & Steinfink (1967) have determined the structure of LaSb$_2$, Gambino (1967) has assigned the

Gd$_4$Bi$_3$ (anti-Th$_3$P$_4$) structure to La$_4$Sb$_3$, and Rieger & Parthé (1968) have recently assigned the Mn$_5$Si$_3$ structure to La$_5$Sb$_3$. The structure determination of La$_2$Sb was undertaken as part of a reinvestigation of the La–Sb system which is still underway (Mansey, Sato, Taylor & Calvert, to be published).

Experimental

La$_2$Sb was prepared as described by Sato, Taylor & Calvert (1967) (La > 99.8, Sb $> 99.99\%$; total impurities in the alloy were found to be in the range 0.05–0.5% by semi-quantitative spectroscopic analysis). The single

* N.R.C. Postdoctoral Fellow.
† Present address: Applied Chemistry, Faculty of Technology, Gunma University, Kiryu, Gunma, Japan.
‡ N.R.C. No. 11,551.

crystals studied came from a pellet of composition La$_2$Sb which was annealed for 2 days at 1100°C *in vacuo* and slowly cooled. The powder data were from a sample of composition La$_2$Sb (annealed for 8 days at 750°C, air-cooled). Precession photographs (Mo $K\alpha$ radiation, Zr filter) of nets *h0l, h1l, 0kl, 1kl, hk0, hk1, hk2, hk4, hk5, hhl* and two general *hkl* nets were recorded; some nets were recorded from two further specimens to check the space group and axial dimensions. Multiple-film zero-level Weissenberg photographs (Cu $K\alpha$ radiation, Ni filtered) of the *hhl* net of the best crystal were used to obtain intensity data for 35 *hhl* reflexions (45

reflexions accessible). The intensities were estimated visually and corrected for Lorentz and polarization effects. Later, when these data had been found to be unsatisfactory, three much smaller crystals were checked (precession photographs) and levels *h0l* and *h1l* were recorded by the multiple-film (interleaved brass foils) Weissenberg technique from a crystal 0·05 × 0·12 × 0·12 mm in size using Zr-filtered and radiation; 144 out of 232 accessible *h0l* reflexions and 154 out of 215 accessible *h1l* reflexions were measured. Intensities were estimated visually, against a scale prepared from the same crystal, and corrected for the Lp effect and absorption

Table 1. *Atomic parameters for* La$_2$Sb

|	Cu radiation	Mo radiation		Weighted mean
	$z(hhl)$ (σ)	$z(h0l)$ (σ)	$z(h1l)$ (σ)	z(final) (σ)
La(1)	0	0	0	0
La(2)	0·32024 (65)	0·32052 (33)	0·32039 (24)	0·32042 (19)
Sb	0·13838 (70)	0·13736 (36)	0·13785 (31)	0·13771 (22)
	B(hhl) (σ)	*B(h0l)* (σ)	*B(h1l)* (σ)	*B*(final) (σ)
La(1)	0·72 (15)	0·670 (79)	0·788 (71)	0·73 (5)
La(2)	0·67 (17)	0·477 (63)	0·352 (53)	0·42 (4)
Sb	1·10 (20)	0·409 (76)	0·433 (64)	0·46 (5)
	(hhl)	*(h0l)*	*(h1l)*	
	45	232	215	Reflexions Accessible
	35	144	154	Observed
	27	133	142	Refined
	0·078	0·134	0·131	*R* value
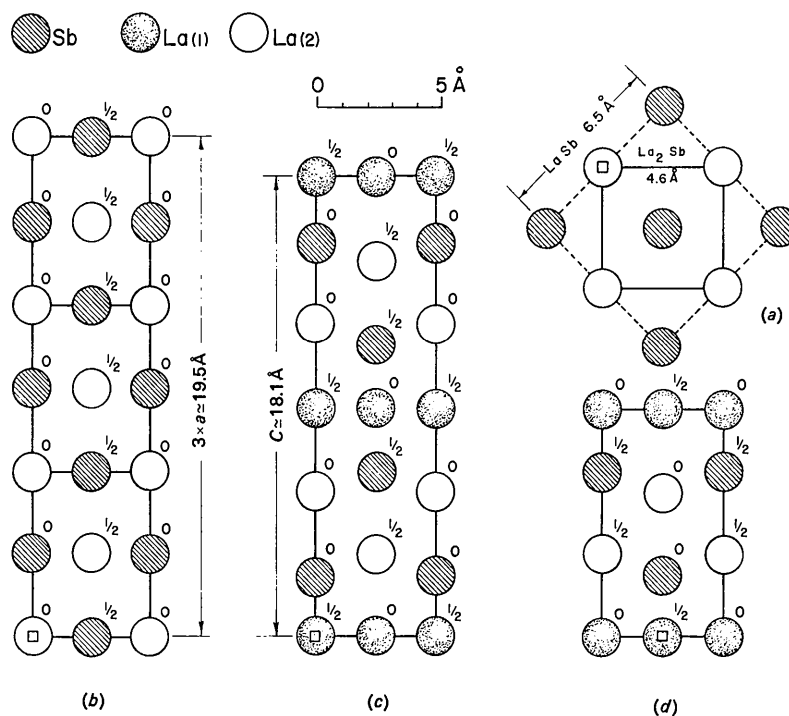
Fig. 1. Structural relationships between LaSb, La$_2$Sb and *C*38 type structures. The figures beside the atoms are fractional heights. The small square marks the origin of the La$_2$Sb cell in each projection. (*a*) Projection along the [001] axis of LaSb (*B*1 type). (*b*) Three LaSb cells stacked together; projection along [110] of LaSb (*B*1 type). (*c*) Projection along [100] in tetragonal La$_2$Sb. (*d*) Projection along [100] in tetragonal *C*38 type.

assuming a sphere of radius 0·056 mm. The internal consistency of the F values was assessed by comparing the 17 available symmetry-related reflexions (10l and 01l) for which $R_{internal} = \sum|\Delta F|/\sum\langle F\rangle$ was 0·15. The lattice parameters were measured on 30° precession photographs ($\lambda K\alpha_1 = 0.7092$ Å) of the crystal used for the intensity measurements. There is evidence from powder photographs of a very small variation in the lattice parameters. The powder pattern given in Table 4 is indexed on parameters $a = 4.636$ ($\sigma = 3$) and $c = 18.11$ ($\sigma = 2$) Å, and was recorded in an 11·46 cm Debye–Scherrer camera using monochromatized Cu $K\alpha$ radiation ($\lambda\alpha_1 = 1.5405$ Å); low angle cut off 14 Å; $t = 25°$C. The I_{calc} values are peak intensities derived from integrated intensities by use of the curve of Swanson, Morris, Stinchfield & Evans (1962). The integrated intensities were calculated for the following parameters: La(1), $B = 0.73$ Å²; La(2), $z = 0.32045$ $B = 0.41$ Å²; Sb, $z = 0.13760$, $B = 0.42$ Å², using a program of Smith (1967) suitably revised for an IBM 360. Values of I_{obs} were obtained by visual comparison with a scale prepared in a powder camera.

Crystal data

La₂Sb, F.W.399·60, tetragonal, $a = 4.626$ ($\sigma = 3$) and $c = 18.06$ ($\sigma = 2$) Å at 25°C, $c/a = 3.904$, $Z = 4$, $U = 386.5$ Å³, $D_x = 6.87$ g.cm⁻³, μ_l for Mo $K\alpha = 287$ cm⁻¹, μ_l for Cu $K\alpha = 2170$ cm⁻¹. Space group $I4/mmm$ (D_{4h}^{17}) No. 139 based on structure and diffraction symbol $4/mmmI...$; 4 La(1) in 4(c), 0 $\frac{1}{2}$ 0 with $B = 0.73$ ($\sigma = 5$) Å²; 4 La(2) in 4(e), 0 0 z with $z = 0.32042$ ($\sigma = 19$) and $B = 0.42$ ($\sigma = 4$) Å², 4 Sb in 4(e), 0 0 z with $z = 0.13771$ ($\sigma = 22$) and $B = 0.46$ ($\sigma = 5$) Å².

The extreme values of the cell dimensions obtained by indexing the back-reflexion lines on powder patterns were $a = 4.636$ ($\sigma = 2$), $c = 18.11$ ($\sigma = 2$) Å, $c/a = 3.906$ and $a = 4.630$ ($\sigma = 1$), $c = 18.062$ ($\sigma = 3$) Å $c/a = 3.901$ at 25°C (Cu $K\alpha_1 = 1.5405$ Å); these patterns are detectably different in the back-reflexion region when compared visually.

Trial structure and refinement

The trial structure was derived from that of LaSb (NaCl, $B1$ type) by noting first that a is equal to half the face-diagonal for LaSb (4·63 Å × 2 ≃ 6·5 Å × √2) [Fig. 1(a)] and secondly that c is slightly less than three times the a dimension for LaSb (18 Å ≃ 3 × 6·5 = 19·5 Å, [Fig. 1(b), (c)]. The composition La₂Sb is obtained by changing one out of every 3 layers from La+Sb to La+La and a reduction in the c dimension is then achieved by shifting the La layers by $a/2$ parallel to a. If the mixed atom planes are buckled, reasonable calculated structure factors are obtained.

At first the copper radiation data hhl could not be refined because the 11l reflexions calculated much too large for the models tried. Extinction was thought to be a possible cause of these discrepancies, although it had

not been considered to be important in the first instance because the crystal had a noticeable mosaic structure. By eliminating the low order 11l reflexions the trial structure was readily refined, using a block-diagonal structure-factor least-squares program which minimized $\sum w(|F_o| - |F_c|)^2$ (Ahmed, 1966); the σ values were also calculated by this program.

The reflexions reduced appreciably by extinction were removed by using a test on $|\Delta F| = |F_o| - |F_c|$. This test removed from the least-squares calculations all reflexions having an $|\Delta F|/F_o$ value greater than some predetermined number T. This quantity was taken to be

Table 2. Observed and calculated structure factors (× 10) for La₂Sb

The F_c values for $h0l$ and $h1l$ were calculated separately from the parameters given in columns 3 and 4 of Table 1. The effects of anomalous dispersion are included in the values of $|F_c|$, but the phase angles were restored to 0 or π during print-out.

[Table of observed and calculated structure factors — dense multi-column numerical data]

* Unobserved, F_o is value of local threshold.
▲ $|\Delta F|/F_o > 0.40$.
⊛ Unknown F_o, back-stop interfered; F_o is value of local threshold.

approximately three times $R_{internal}$, the internal consistency in the F_o data. On the assumption that the errors in F_o have a normal distribution and that $R_{internal} \simeq \sigma(F_o)$, a valid F_o will be rejected by this test less than 1 % of the time, provided that the model for F_c is correct. In the present case, use of this test gave a rapid convergence using F_o data which had previously not been successfully refined. Use of such a test obviously requires caution, but is satisfactory when the parameters are adequately determined and there is good reason to believe in the model.
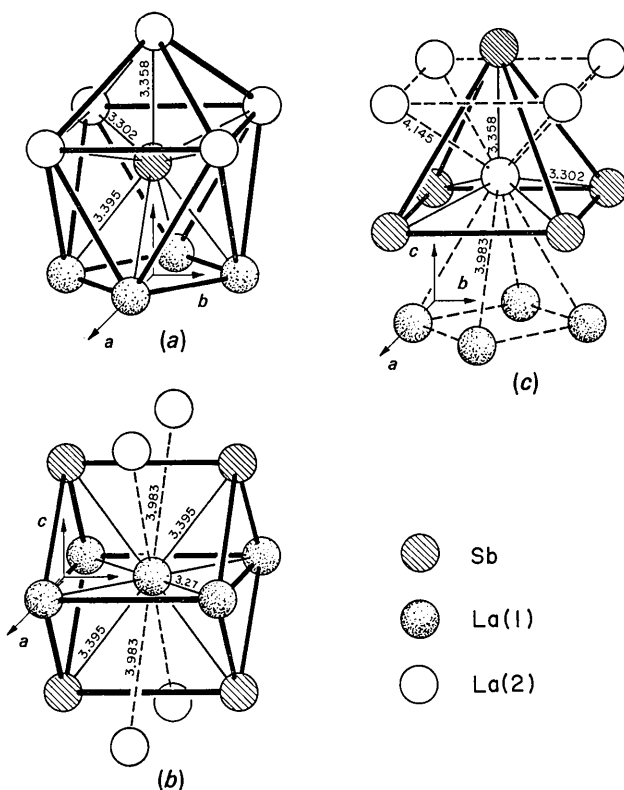

Fig. 2. Atomic coordinations in La₂Sb. Solid lines for nearest neighbours, broken lines for next-nearest neighbours. (a) Sb atom at 0, 0, 0·138 (0 0 z), (b) La (1) atom at 0, ½, 0, (c) La (2) atom at ½, ½, 0·180 (½, ½, ½ - z).

Rather than attempt corrections for extinction and to continue the refinement, it appeared better to collect a more extensive set of data from a different crystal with Mo radiation. A preliminary analysis of this data revealed some extinction and absorption effects, both considerably reduced, however, as well as discrepancies tentatively attributed to multiple-reflexion (e.g. 204 with a possible contribution from $\overline{4}00$).

Following this preliminary analysis, the two sets of reflexions $h0l$ and $h1l$ were refined separately using the structure-factor least-squares program described above with $T = 0\cdot40$. Isotropic temperature factors were used, all observed planes were given unit weight and scattering factors (TFD, International Tables for X-ray Crystallography, 1962) were corrected for dispersion ($\delta f'$ and $\delta f''$). The refinements were considered complete when the final shifts were less than 10 % of the σ values. The results are given in Tables 1,2 and 3.

Comparison of the results obtained from the separate refinements of $h0l$ and $h1l$ gave a check on the accuracy of the overall procedure. It was possible that the results might have been affected by the experimental errors but unlikely that these would have equal effect in both zones. The results are subject to the criticism that the parameters are a function of the unit weighting scheme used. To test this, the $h0l$ data were refined, using weights $\sqrt{w} = 1/\{1 + [(|F_o| - P_2)/P_1]^2\}^{1/2}$ with $P_1 = 13$ and $P_2 = 45$ which gave nearly constant, but not unit values for $\sum w|\Delta F|^2/N$, where N is the number of reflexions in small ranges of $\sin^2 \theta$ and F_o. No test on $|\Delta F|$ was applied and hence all observed reflexions were included in the refinement. The results obtained for the positional parameters [La(2), $z = 0\cdot32043$ ($\sigma = 13$); Sb, $z = 0\cdot13740$ ($\sigma = 15$)] are substantially identical, with σ values smaller than before by about 50 % (see Table 1); the thermal parameters have increased while the corresponding σ values have decreased [La(1), $B = 0\cdot96$ ($\sigma = 3$) Å²; La(2), $B = 0\cdot73$ ($\sigma = 3$) Å²; Sb, $B = 0\cdot72$ ($\sigma = 3$) Å²]. Thus the positional parameters of Table 1 are adequately determined but the temperature parameters are less accurate, although of the right order. Lower σ values could undoubtedly be obtained by a combined refinement of the $h0l$ and $h1l$ data with appropriate weights, but this was not essential for the pres-

Table 3. Interatomic distances in La₂Sb

(σ includes uncertainty in unit-cell dimensions)

Atom and symmetry	Neighbours	Distances (Å)					
		(h0l)	(σ)	(h1l)	(σ)	weighted mean	(σ)
La(1)	4 La (1)	3·271	(3)	3·271	(3)	3·271	(2)
mmm	4 La(2)	3·982	(6)	3·984	(5)	3·983	(4)
	4 Sb	3·392	(6)	3·398	(5)	3·395	(4)
La(2)	4 La(1)	3·982	(6)	3·984	(5)	3·983	(4)
4mm	4 La(2)	4·146	(6)	4·143	(5)	4·144	(4)
	1 Sb	3·358	(4)	3·357	(4)	3·357	(3)
	4 Sb	3·308	(9)	3·297	(7)	3·302	(6)
Sb	4 La(1)	3·392	(6)	3·398	(5)	3·395	(4)
4mm	1 La(2)	3·358	(4)	3·357	(4)	3·357	(3)
	4 La(2)	3·308	(9)	3·297	(7)	3·302	(6)

ent purpose. The mean interatomic distances (Table 3) are all within $1·0\,\sigma$ of the independent values from the $h0l$ and $h1l$ data, indicating that the estimates for σ are of the right order.

An overall check of the correctness of this structure was now made by calculating the powder pattern (Table 4). The observed powder intensities could be expected to be substantially free from extinction, the absorption could be adequately corrected because the specimen was cylindrical and multiple reflexion should affect the results much less because of the random orientation of the powder particles. The good overall agreement is indicative of an adequately refined structure (Smith, 1968). Table 2 includes 23 weak reflexions excluded from the least-squares refinement by the test on $|\Delta F|$. These are about equally divided between low-angle reflexions with $|F_o| > |F_c|$ and high-angle reflexions with $|F_o| < |F_c|$. The error analysis results (Ahmed & Barnes, 1963) were of the form usually observed with the photographic method. The larger discrepancies are observed at the lower and higher angles and also with the smaller and larger $|F_o|$ values. The analysis of the $|\Delta F|$ values for the unobserved planes, which were not used in the least-squares refinement, shows a normal distribution with about 1 % having a $|\Delta F|$ greater than $2F_{\text{threshold}}$ ($F_{\text{threshold}}$ calculated from I_{obs} (minimum) $\times 0·6$).

The final values listed in column five of Table 1 and column five of Table 3 are weighted means ($w_i = 1/\sigma_i$). Further refinement with anisotropic temperature factors was not undertaken in view of the approximate absorption correction.

Alternative structures

Lanthanum and antimony have very similar scattering powers and it is possible to formulate other arrangements of the atoms in the same sets of positions. The arrangements listed in Table 5 were refined by the least-squares method described above but in this case includ-

ing all observed reflexions in the calculation in order to keep the total number of reflexions constant. The significance of the changes in R (based on observed planes only) was examined by Hamilton's (1965) R test. The refinement included 6 parameters ($K, B_{\text{La}}, B_{\text{La}}, B_{\text{Sb}}, z_1, z_2$) so that there were 138 and 148 degrees of freedom for $h0l$ and $h1l$ respectively. The results are listed in Table 6. Structures (II) and (III) can be safely rejected at the 0·005 level with both sets of data. Hence structure (I) was accepted as having the correct arrangement of atoms.

Table 4. *Powder X-ray diffraction pattern of* La₂Sb
(see text)

d_obs	d_calc	h	k	l	I_obs	I_calc	d_obs	d_calc	h	k	l	I_obs	I_calc
3.23	3.28	1 1 0			<22	13	1.040	1.043	2 1 15			<22	16
3.03	3.08	1 1 2			66	100	1.034	1.038	1 0 17			66	13
2.97	3.02	0 0 6			42	42		1.037	4 2 0				65 49
2.81	2.85	1 0 5			42	39		1.035	3 0 13				3
2.62	2.66	1 1 4			82	110	1.029	1.032	4 0 8			<22	13 3
2.29	2.32	2 0 0			82	95		1.031	4 1 7				10
2.23	2.26				22	3	1.015	1.017	2 0 16			26	26 23
	2.26	1 0 7				24 20		1.015	2 2 14				3
	2.25	2 0 2				1	1.011	1.013	3 2 11			42	43
1.85	1.86	1 1 8			26	23	.978	.981	4 1 9			66	68 8
1.82	1.85	1 0 9			82	11		.980	4 2 6				60
	1.84	2 0 6				93 82	.968	.970	3 1 14			26	16
1.78	1.80	2 1 5			34	40	.958	.962	1 1 18			26	17
1.63	1.64	2 2 0			42	54	.945	.948	2 1 17			34	26
1.61	1.62	2 0 8				7	.929	.931	2 2 16			22	23
	1.62	2 1 7			34	29 21	.927	.929	4 1 11			52	45
	1.61	2 2 2				1	.918	.919	4 0 12			<22	6
1.575	1.585	1 1 10			26	21	.908	.909	5 1 0			<22	6
1.539	1.551	1 0 11			42	41	.903	.905	5 1 2			42	38
1.456	1.466	3 1 0			<22	9	.897	.900	2 2 10				4
1.435	1.447				82	62		.898	5 0 5			42	30 9
	1.444	2 1 9				128 14		.898	3 3 9				17
	1.440	2 2 6				52	.891	.891	5 1 4			66	51
1.413	1.427	2 0 10			22	17 4	.879	.880	3 2 15			<22	19
	1.421	3 0 5				13	.876	.877	3 0 17			<22	14
1.386	1.395	3 1 4			66	77	.8715	.8728	5 0 7				6
1.363	1.371	1 1 12			<22	7		.8728	4 3 7			26	38 11
1.318	1.327	2 2 8			<22			.8728	1 1 20				21
	1.326	3 0 7				12 7	.8537	.8545	4 2 12			<22	13
1.283	1.294	0 0 14			66		.8429	.8437	5 1 8			26	19
	1.289	2 1 11				59 1	.8414	.8421	5 0 9			26	15 5
1.255	1.265	2 0 12			<22	58		.8421	3 3 9				10
1.224	1.231	3 1 18			22	8	.8375	.8376	5 2 5			22	20
1.209	1.215	2 2 10			22	20	.8348	.8348	3 3 14			22	10
	1.212	3 2 5				22 3 19	.8290	.8296	3 1 18			52	43
1.198	1.203	1 1 14			<22	10	.8225	.8232	0 0 22			52	37 15
1.164	1.168	1 0 15			<22	10		.8228	4 1 15				22
1.155	1.159	4 0 0			<22	26 8	.8195	.8203	3 2 17			82	65 33
	1.156	2 1 13				36 8		.8195	4 4 0				32
1.146	1.151	3 2 7			<22	11	.8169	.8169	5 2 7			42*	13
1.136	1.139	3 1 10			22	22	.8123	.8125	5 1 10			42	25
1.123	1.130	2 0 14			26	26 3	.8095	.8098	4 0 16			34	30
1.079	1.127	0 0 11				23	.8074	.8079	4 3 11			128	92 61
	1.085	3 3 2			42	19		.8079	5 0 11				31
	1.083	3 2 9				60 9	.7918	.7920	5 3 2			-52	54
	1.082	4 0 6				32	.7907	.7909	4 4 6			42	45
1.070	1.074	4 1 5			22	16	.7831	.7831	5 3 4			102	79
1.058	1.062	3 3 4			26	24	.7788	.7788	5 1 12			22	16
1.050	1.052	3 1 12			<22	10	.7756	.7757	2 0 22			102	103

* α_2 overlap major contribution.

Table 5. *R values for different atomic arrangements in* La₂Sb

	I4/mmm			R value	
Structure	4(c) 0½0	4(e) 00z₁	4(e) 00z₂	(h0l)	(h1l)
I	La(1)	La(2)	Sb	0·149	0·140
II	La(1)	Sb	La(2)	0·163	0·163
III	Sb	La(2)	La(1)	0·157	0·151
IV	La(1) (0·95)	La(2)	Sb	0·147	0·139

Table 6. *Comparison of different atomic arrangements in* La₂Sb

Structures	(h0l)	(h1l)
II vs. I	$R_{II}/R_I = 1·094$	$R_{II}/R_I = 1·164$
	$\mathscr{R}_{1,\,138,\,0·005} < 1·034$	$\mathscr{R}_{1,\,148,\,0·005} < 1·034$
III vs. I	$R_{III}/R_I = 1·054$	$R_{III}/R_I = 1·079$
	$\mathscr{R}_{1,\,138,\,0·005} < 1·034$	$\mathscr{R}_{1,\,148,\,0·005} < 1·034$
I vs. IV	$R_I/R_{IV} = 1·014$	$R_I/R_{IV} = 1·007$
	$\mathscr{R}_{1,\,137,\,0·10} < 1·011$	$\mathscr{R}_{1,\,147,\,0·25} < 1·006$

In structure (I) the La(1) atoms lie in densely packed planes. This type of plane in the related structure of NdTe$_{1\cdot80}$ (Wang, Steinfink & Bradley, 1966) has been shown to have vacancies. In addition the unit-cell parameters for La$_2$Sb as derived from different X-ray powder diffraction patterns have slightly different values. Hence the occupancy factor for the La(1) atom was refined. Starting with a value of 0·5, the final occupancy factor was found to be 0·95. For this refinement [structure (IV)] the R values for the ($h0l$) and ($h1l$) data are given in Table 5. The change in R [with respect to structure (I)] was examined by Hamilton's R test. The results shown in Table 6 do not compel the rejection of structure (I), since the probability of error in rejection would be 10 to 25%. The occupancy factor for La(1) was therefore taken as unity.

Description of the La$_2$Sb structure

A projection of the La$_2$Sb structure along the a axis is shown in Fig. 1(c), while the arrangement of nearest neighbours and next-nearest neighbours for each atom is illustrated in Fig. 2.

The eight nearest neighbours of the La(1) atom lie at the corners of a cube, slightly distorted by extension along the La$_2$Sb [001] direction [Fig. 2(b)]. The La–Sb distances of 3·39 Å are quite normal, but the La(1)–La(1) distances of 3·27 Å are noticeably shorter than the free-metal contact distances (3·73 and 3·77 Å). There are also next-nearest neighbours, four La(2) at 3·98 Å, making a total coordination of 12.

The nearest neighbours of the La(2) atoms [Fig. 2(c)] are Sb atoms arranged at the corners of a square pyramid, which is a distinctive feature of the La$_2$Sb and related (C38) structures and will be discussed briefly below. The distances are 3·36 Å to the atom at the vertex of the pyramid and 3·30 Å to the four Sb atoms at the corners of the square base. There are also eight next-nearest neighbours, four La(1) atoms at 3·98 Å and four La(2) atoms at 4·15 Å, making a total coordination of 13.

The Sb atom [Fig. 2(a)] has nine nearest neighbours forming a mono-capped square antiprism with distances ranging from 3·30 to 3·40 Å. An alternative description for this arrangement is as a trigonal prism with; 1 La(1) + 2 La(2) forming each end face with three extra atoms, 2 La(1) + 1 La(2), opposite the prism faces. This coordination occurs widely for the B group atoms, in their transition metal compounds, e.g. Co$_2$P and Ta$_2$P.

The La$_2$Sb structure belongs to a fairly diverse group of structures of the metal-rich compounds between transition metals and chalcogenides or pnictides. These structures are characterized by metal–metal bonds and nearest neighbour coordinations of less than 12, in this case 8, 5 and 9 as compared with total coordination numbers of 12, 13 and 9.

Finally it may be noted that the structure of Ti$_2$Bi (Auer-Welsbach, Nowotny & Kohl, 1958) is in fact analogous to that derived here for La$_2$Sb. The structure assigned to Ti$_2$Bi places 2 Ti in 2(a), 0 0 0; 2 Ti in 2(b), $\frac{1}{2}$ $\frac{1}{2}$ 0; 4 Ti in 4(i), 0 $\frac{1}{2}$ 0·133, 4 Bi in 4(i), 0 $\frac{1}{2}$ 0·353, in the space group $P4_2/mmc$ (D_{4h}^9) No. 131. By first adding $\frac{1}{2}$ to all y coordinates (*i.e.* shifting the origin to $-b/2$) and then combining the Ti atoms in 2(a) with those in 2(b) we get the position 4(c) in $I4/mmm$. Similarly the positions 4(i) convert to 4(e) of $I4/mmm$. Thus the correct space group for the Ti$_2$Bi structure is $I4/mmm$.

Comparison of La$_2$Sb with C38 and $E0_1$ structures

The close-packed plane of La(1) atoms in La$_2$Sb prompted a geometrical study of the A_2B (C38) type structures. The occurrence of such layers in the similar structures of NdTe$_2$ (C38) and NdTe$_3$ has been discussed in terms of their electrical properties (Wang, Steinfink & Bradley, 1966; Norling & Steinfink, 1966).

The C38 structure is formally and geometrically equivalent to the $E0_1$ structure [Pearson (1965) gives data for these structure types]. This may be seen by tabulating a, c and c/a values and by calculating the interatomic distances and coordinations. It is convenient here to use the C38 structure as the reference. The reported structure for Cu$_2$Sb, commonly quoted as representative of the C38 type, is atypical in that the buckling of the mixed atom planes is reversed, with Cu atoms moving out of the mixed atom plane towards the all-Cu plane.

The most typical feature of the C38 structure is found to be the square pyramidal coordination of five generally larger B atoms around the A atom [Fig. 2(c)]. Both the a and c axial lengths are largely determined by the A–B distance in this pyramid in which the vertical and sloping distances are approximately equal. It may be noted that those A_2B (C38) compounds that involve metals of the first long period have small c/a ratios ($< 1\cdot80$), while those that involve metals of the second (and higher) long periods have large c/a ratios ($> 2\cdot00$). The radius ratios r_A/r_B (12 C.N.) in the A_2B compounds are (generally) $0\cdot85 \pm 5$ and as a direct consequence the layer composed solely of A atoms [Fig. 2(b)] is usually not close-packed. Where the ratio is significantly greater than $1\cdot0$ the A atoms in this layer come into contact and the extreme example occurs with La$_2$Sb for which $r_A/r_B = 1\cdot15$. It appears that the five La–Sb contacts in the square pyramid provide enough energy to compress the La(1) atoms by about 12%.

Thus the La$_2$Sb structure is comparable to the C38 type in that the La–Sb contacts in the pyramid largely determine the a and c axes. The large r_A/r_B ratio of $1\cdot15$ for La$_2$Sb, implying a pronounced compression of the La(1) atoms is, however, not characteristic of most C38 structures.

References

AHMED, F. R. (1966). N.R.C. Crystallographic Programs for the IBM/360 system. Data Reduction and Structure Factor Least Squares.

AHMED, F. R. & BARNES, W. H. (1963). *Acta Cryst.* **16**, 1249.

AUER-WELSBACH, H., NOWOTNY, H. & KOHL, A. (1958). *Mh. Chem.*, **89**,154.

GAMBINO, R. J. (1967). *J. Less-Common Met.* **12**, 344.

HAMILTON, W. C. (1965). *Acta Cryst.* **18**, 502

IANDELLI, A. & BOTTI, F. (1937). *Atti reale Acad. nazl. Lincei*, **25**, 498.

International Tables for X-ray Crystallographic (1962). Vol. III. pp. 211, 213. Birmingham: Kynoch Press.

NORLING, B. K. & STEINFINK, H. (1966). *Inorg. Chem.* **5**, 1488.

PEARSON, W. B. (1965). *A Handbook of Lattice Spacing and Structures of Metals and Alloys*, Vol. 2. Toronto: Pergamon Press.

RIEGER, W. & PARTHÉ, E. (1968). *Acta Cryst.* B**24**, 456.

SATO, M., TAYLOR, J. B. & CALVERT, L. D. (1967). *J. Less-Common Met.* **12**, 419.

SMITH, D. K. (1967). Revised program for calculating X-ray powder diffraction patterns. UCRL-50264.

SMITH, D. K. (1968). *Norelco Reporter*, **15**, 57.

SWANSON, H. E., MORRIS, M. C., STINCHFIELD, R. P. & EVANS. E. H. (1962). *Nat. Bur. Stand. Monograph 25* – Section 1,3.

VOGEL, R. & KLOSE, H. (1954). *Z. Metallk.* **45**, 633.

WANG, R. & STEINFINK, H. (1967). *Inorg. Chem.* **6**, 1685.

WANG, R., STEINFINK, H. & BRADLEY, W. F. (1966). *Inorg. Chem.* **5**, 142.

The Crystal Structure of Anhydrous UO₂F₂*

By M. ATOJI AND M. J. McDERMOTT†

Chemistry Division, Argonne National Laboratory, Argonne, Illinois 60439, U.S.A.

A neutron powder-diffraction study of UO_2F_2 has been carried out. The structure is trigonal with a unit-layer unit cell with $a=b=4\cdot192\pm0\cdot001$ and $c/3=5\cdot220\pm0\cdot003$ Å and bonding distances of $U-O=1\cdot74\pm0\cdot02$ and $U-F=2\cdot429\pm0\cdot002$ Å, confirming essentially a previous X-ray study but with considerably higher accuracy. The powder sample consisted of approximately equal cumulative volumes of four different types of *ordered* coherent domains, containing individually the layer sequences, $A^+B^+C^+$, $A^-B^-C^-$, $A^+B^+A^+B^+C^+B^+C^+A^+C^+$ and $A^-B^-A^-B^-C^-B^-C^-A^-C^-$, where $(+)$ and $(-)$ refer respectively to the right-side-up and upside-down unit-layer configurations. In each layer sequence, a backward stacking with the opposite-sign unit layer is equally possible in powder diffractometry. All structures belong to the centric trigonal space group $R\bar{3}m$ (D^5_{3d}). The polymorphic, multidomain structure is not necessarily unique, although an exhaustive search for other probable models was fruitless.

Introduction

Zachariasen (1954) made a pioneering contribution to the structure chemistry of the 5*f* series of elements by solving the crystal structures of a number of actinide compounds using the X-ray diffraction method. His study included anhydrous uranyl fluoride, UO_2F_2, which was found to exhibit growth layer-stacking faults almost inherently (Zachariasen, 1948). Based on the X-ray powder data, Zachariasen assigned a rhombohedral structure with a cubic close-packing layer sequence to the *ideally* ordered UO_2F_2 and interpreted the stacking faults by introducing a hexagonal close-packing sequence with a random-walk

probability. The stacking ordering increases with heat treatment, but the *ideally* ordered structure is hardly achievable in practice. Since neutron diffraction is more sensitive to the structure parameters of UO_2F_2, we have re-examined the subject using this technique. In this paper the rhombohedral crystal structure is conveniently described with reference to hexagonal axes unless otherwise stated.

Experimental

The anhydrous UO_2F_2 used in this work was prepared by treating UO_3 with gaseous anhydrous HF at temperatures between 350 and 500°C in a nickel reactor (Hoekstra, 1963). Chemical analysis of the samples confirmed the stoichiometry, as indicated by a satisfactory agreement between the observed and calculated weight percentages (the latter values in parentheses), uranium $77\cdot1\pm0\cdot1$ (77·28), oxygen $10\cdot3\pm0\cdot1$ (10·39)

---

* Work performed under the auspices of the U.S. Atomic Energy Commission.

† Present address: Imperial Chemical Industries Limited, Petrochemical and Polymer Laboratory, P.O. Box 11, The Heath, Runcorn, Cheshire, England.